48. ZEOLITE AND SILICA DIAGENESIS AND SANDSTONE PETROGRAPHY AT SITES 438 AND 439 OFF SANRIKU, NORTHWEST PACIFIC, LEG 57, DEEP SEA DRILLING PROJECT

Azuma Iijima, Ryo Matsumoto, and Ryuji Tada, Geological Institute, University of Tokyo, Hongo, Tokyo, Japan

ABSTRACT

We detected authigenic clinoptilolites in two core samples of tuffaceous, siliceous mudstone in the lower Miocene section of Hole 439. They occur as prismatic and tabular crystals as long as 0.03 mm in various voids of dissolved glass shards, radiolarian shells, calcareous foraminifers, and calcareous algae. They are high in alkalies, especially Na, and in silica varieties. There is a slight difference in composition among them. The Si : (Al + Fe^{3+}) ratio is highest (4.65) in radiolarian voids, intermediate (4.34) in dissolved glass voids, and lowest (4.26) in voids of calcareous organisms. This difference corresponds to the association of authigenic silica minerals revealed by the scanning electron microscope: There are abundant opal-CT lepispheres in radiolarian voids, low cristobalite and some lepispheres in dissolved glass voids, and a lack of silica minerals in the voids of calcareous organisms. Although it contains some silica from biogenic opal and alkalies from trapped sea water, clinoptilolite derives principally from dissolved glass. Although they are scattered in core samples of Quaternary through lower Miocene diatomaceous and siliceous deposits, acidic glass fragments react with interstitial water to form clinoptilolite only at a sub-bottom depth of 935 meters at approximately 25°C.

Analcimes occur in sand-sized clasts of altered acidic vitric tuff in the uppermost Oligocene sandstones. The analcimic tuff clasts were probably reworked from the Upper Cretaceous terrain adjacent to Site 439.

Low cristobalite and opal-CT are found in tuffaceous, siliceous mudstone of the middle and lower Miocene sections at Sites 438 and 439. Low cristobalite derives from acidic volcanic glass and opal-CT from biogenic silica. Both siliceous organic remains and acidic glass fragments occur in sediments from the Quaternary through lower Miocene sections. However, the shallowest occurrence is at 700 meters sub-bottom in Hole 438A, where temperature is estimated to be 21°C. The $d(101)$ spacing of opal-CT varies from 4.09 to 4.11 Å and that of low cristobalite from 4.04 to 4.06 Å. Some opal-CT lepispheres are precipitated onto clinoptilolites in the voids of radiolarian shells at a sub-bottom depth of 950 meters in Hole 439.

Sandstone interlaminated with Upper Cretaceous shale is chlorite–calcite cemented and feldspathic. Sandstones in the uppermost Oligocene section are lithic graywacke and consist of large amounts of lithic clasts grouped into older sedimentary and weakly metamorphosed rocks, younger sedimentary rocks, and acidic volcanic rocks. The acidic volcanic clasts probably originated from the volcanic high, which supplied the basal conglomerate with dacite gravels. The older sedimentary and weakly metamorphosed rocks and green rock correspond to the lithologies of the lower Mesozoic to upper Paleozoic Sorachi Group, including the chert, limestone, and slate in south-central Hokkaido. However, the angular shape and coarseness of the clasts and the abundance of carbonate rock fragments indicate a nearby provenance, which is probably the southern offshore extension of the Sorachi Group. The younger sedimentary rocks, including mudstone, carbonaceous shale, and analcime-bearing tuff, correspond to the lithologies of the Upper Cretaceous strata in south-central Hokkaido. Their clasts were reworked from the southern offshore extension of the strata. Because of the discontinuity of the zeolite zoning due to burial diagenesis, an overburden several kilometers thick must have been denuded before the deposition of sediments in the early Oligocene.

INTRODUCTION

Research on zeolite diagenesis and sandstone petrography has been done on the Cenozoic and Upper Cretaceous sediment samples collected by the *Glomar Challenger* from Sites 438 and 439 during Leg 57. The two sites are situated in the uppermost part of the inner slope of the Japan Trench off Sanriku about 150 km east of Hachinohe, northeast Honshu (Figure 1). The samples were selected from four holes: Hole 438, at 40°37.75′N, 143°13.90′E, with a water depth of 1552 meters; Hole 438A, at 40°37.79′N, 143°14.15′E, with a water depth of 1558 meters; Hole 438B, at 40°37.80′N, 143°14.80′E, with a water depth of 1564.5 meters; and Hole 439, at 40°37.61′N, 143°18.63′E, with a water depth of 1656 meters. Their stratigraphic position and sub-bottom depth are shown in Figure 2.

In Part I of this chapter the occurrence and properties of zeolites and related silica minerals are described and their origin discussed with reference to the zeolitic burial diagenesis in adjacent Northern Japan. Part II describes the petrography of sandstones on the basis of thin section analyses and considers their provenance with reference to the paleogeology of Hokkaido and zeolite diagenesis.
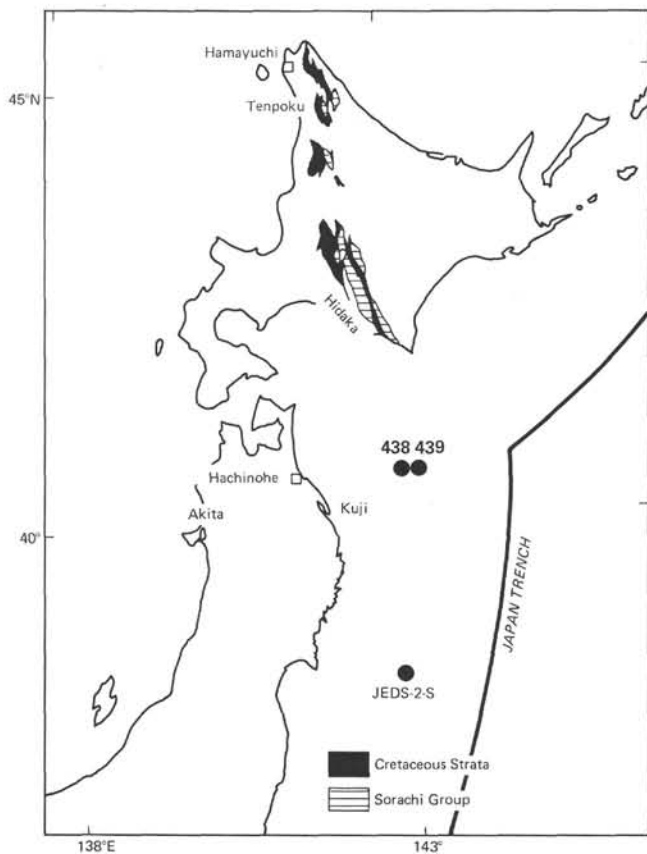

Figure 1. *Location map of Sites 438 and 439, DSDP Leg 57. JEDS-2-S is the site researched by the* Ryofumaru.

PART I. ZEOLITE DIAGENESIS

A total of 137 selected core samples, 100 from Site 438 and 37 from Site 439, were studied by means of X-ray diffraction powder analysis. Thin sections of 18 core samples were observed under a polarizing micro-
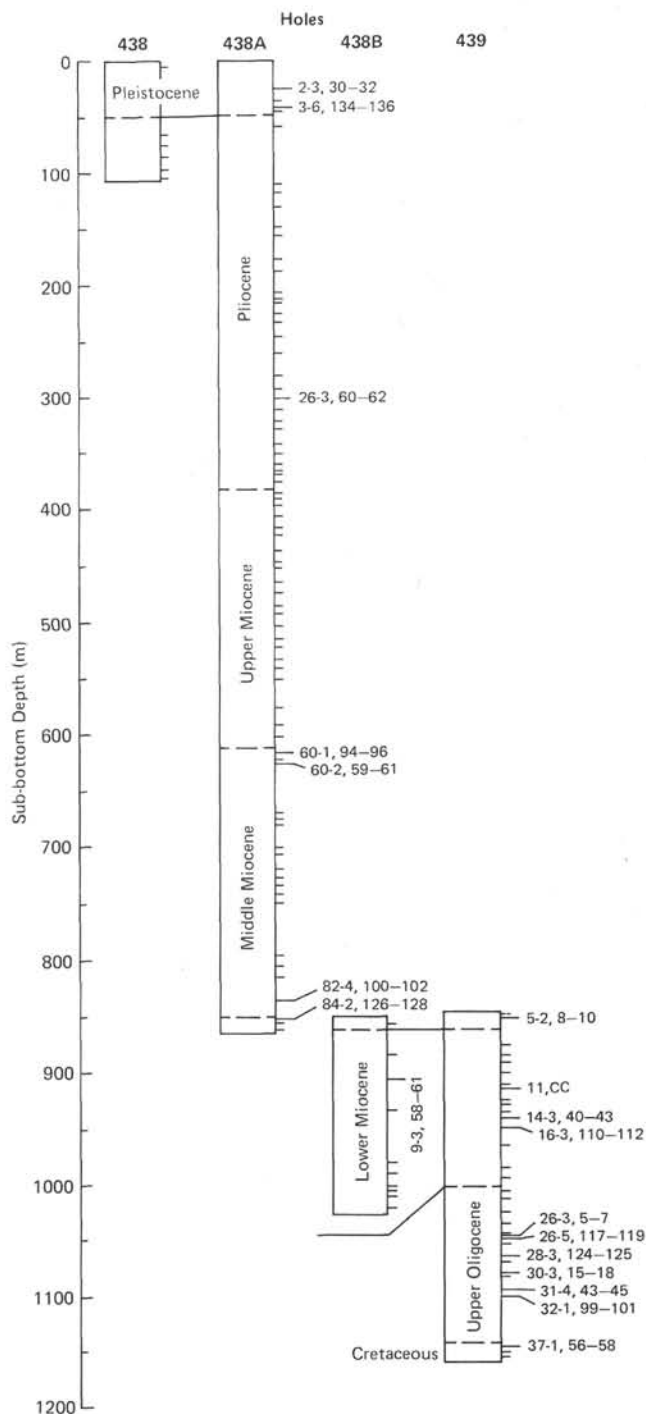

Figure 2. *Stratigraphy of core samples analyzed, according to shipboard scientific results. (Intervals are in cm.)*

scope. Authigenic clinoptilolite was found in two tuf-faceous, siliceous mudstone samples from the lower Miocene section at Site 439. In addition, detrital analcime was discovered in three lithic sandstone samples from the uppermost Oligocene section at Site 439.

Mode of Occurrence of Zeolites

Authigenic Clinoptilolite

Authigenic clinoptilolite was identified in two core samples collected from Hole 439 at a sub-bottom depth of 935 meters (439-14-3, 40–43 cm) and 950 meters (439-16-3, 110–112 cm), the depth interval in the upper part of the lower Miocene section. The two samples are tuffaceous, sandy, siliceous mudstone: 439-14-3 is light gray and rather soft, and 439-16-3 is light buff-gray and tough. Angular clastic grains as large as 0.25 mm in diameter and various organic remains are scattered in a fine matrix consisting of opaline silica, pale green montmorillonitic clay, and pale brown organic pigments with minute illite flakes (Figure 3A). Small, irregularly shaped clay patches are randomly distributed, probably produced by bioturbation. Crystal fragments consist of abundant quartz and fresh plagioclase ($An_{20}Ab_{80}$–$An_{50}Ab_{50}$), a small quantity of biotite and chlorite, and rare zircon and epidote. Lithic fragments consist of abundant acidic glassy rocks with plagioclase laths and a small amount of chert. Altered volcanic glass fragments less than 0.15 mm in size with a bubble-wall structure, are not uncommon. Siliceous organic remains are common. From their size—0.04 to 0.08 mm in diameter—we may infer that thin opaline rings are dissolved diatom frustules. The opaline matrix of the siliceous mudstone may derive from diatom frustules. Spherical and elliptical radiolarian shells 0.1 to 0.5 mm in diameter are not uncommon. They retain their original structure, though they are recrystallized into an aggregate of opal-CT. Sponge spicules with a central canal are also not uncommon. Though uncommon, calcareous tests of foraminifers are well preserved, with open chambers. Well-preserved remains of calcareous echinoid spines are abundant in Sample 439-14-3. A thick, porous wall encloses a central void whose round cross section is 0.04 to 0.06 mm in diameter, the pores of the wall are partly filled with sparry calcite. Brown to black carbonaceous fragments less than 0.1 mm long are uncommon and rarely retain their cellular structure.

Clinoptilolites are present in 2 to 3 per cent of the samples. They occur as fillings in voids of dissolved glass shards, radiolarian shells, and such calcareous microorganisms as echinoids and foraminifers. Fine-grained vitric shards are completely replaced by an aggregate of microcrystalline clinoptilolites which is fringed with a film of smectite and low cristobalite (Figure 3B). Prismatic and tabular clinoptilolites less than 0.02 mm long grow on the wall of the void of dissolved shards (Figure 3C). In the voids of radiolarian shells, clinoptilolites occur on siliceous shells as prismatic and tabular crystals as long as 0.03 mm long (Figure 3D). Clinoptilolites with similar habits and dimensions also fill the cham-

bers of calcareous tests of foraminifers and the central voids of calcareous spines (Figure 3E).

The scanning electron microscope (SEM) reveals some interesting features. All samples were observed on a fractured surface which had been cleaned in water, using ultrasonic waves, then coated with Au–Pd and carbon. Some clinoptilolites have such sharp corners and edges and such flat surfaces that no dissolution phenomena can be considered. In the voids of radiolarian shells, clinoptilolites and equigranular lepispheres 2.5 to 3.5 μm in diameter cover the walls (Figure 4A and B). They are composed of an aggregate of numerous rods 0.6 to 1 μm long (Figure 4C and D). Their morphology and mode of occurrence correspond to those of the opal-CT lepispheres reported by Oehler (1975). They grow on the surfaces of clinoptilolite crystals, and opal-CT sometimes forms a hemilepisphere or a mushroom-like lepisphere (Figure 4A and D). In the voids of dissolved glass shards, clinoptilolites grow on walls 2-μm-thick which are covered with a mosslike aggregate of numerous tiny needles of low cristobalite (Figure 5A and B). Lepispheres and hemilepispheres 3 μm in diameter also grow on the clinoptilolite crystals (Figure 5A and B). However, it is not certain whether the lepispheres in the voids of dissolved glass shards are opal-CT or low cristobalite. No lepispheres coexist with clinoptilolites in the void of calcareous spines.

Detrital Analcime

Clasts of altered acidic tuff are sparse but persistent in Hole 439 samples at a sub-bottom depth of 1063 to 1091 meters in the uppermost Oligocene sandstone section. They occur as subangular to subrounded, medium to coarse, sand grains. The tuff, which exhibits vitroclastic texture, consists principally of fine-grained glass fragments with a bubble-wall structure. It contains rare biotite, quartz, and fresh plagioclase in the form of pyrogenic crystal fragments. The glass fragments are completely altered to pale green chlorite, microcrystalline quartz, and isotropic analcime (Figure 3F). This alteration undoubtedly took place before the tuff was eroded and deposited as clasts, because large amounts of dacite clasts with unaltered or slightly altered glass coexist with the analcimic tuff clasts in the sandstones.

Properties of Authigenic Clinoptilolites and Related Silica

Clinoptilolites

Chemical Composition

Polished thin sections of two clinoptilolite-containing samples (439-14-3 and 439-16-3) were examined with a JXA-5 electron microprobe analyzer at the Geological Institute, University of Tokyo. Volatilization of light elements was reduced by using low sample currents of 0.018 μA on periclase at 15 kv, a beam diameter of 5 μm, and a 4-s exposure. The correction is after the method of Bence and Albee (1968). Counts of Si, Al, Fe, Mg, Ca, and K on 2-, 4-, 8-, 10- and 20-s exposures
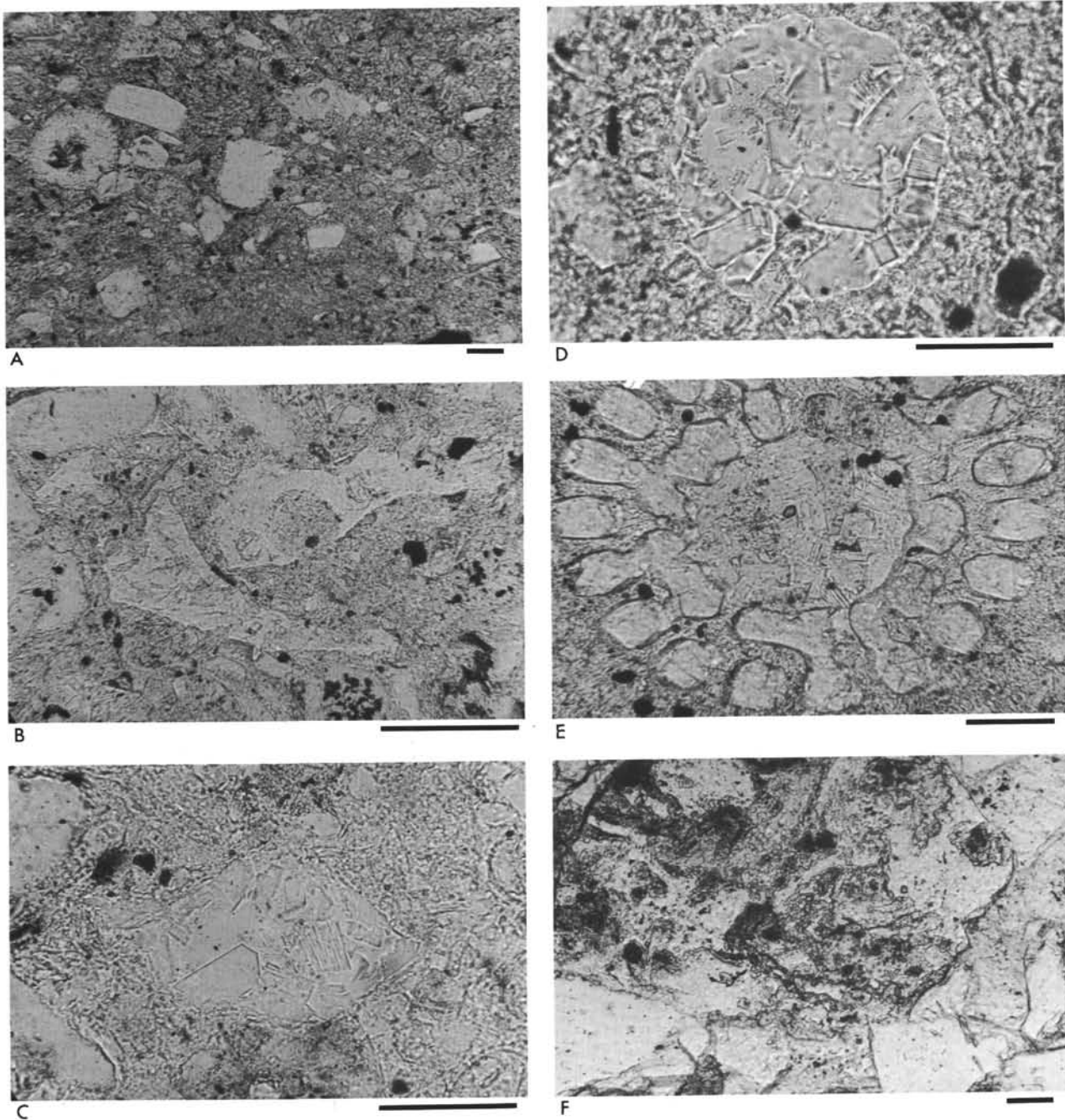
Figure 3. *Micrographs showing authigenic clinoptilolites and detrital analcime. (Each scale bar represents 0.05 mm; unpolarized light.) A. (Sample 439-16-3, 110–112 cm) Tuffaceous, siliceous mudstone containing clinoptilolites and plagioclase, glass fragments, radiolarian shells, and diatom frustules. (Lower Miocene section at a sub-bottom depth of 950 meters in Hole 439.) B. (Sample 439-16-3) Acidic glass shards replaced by an aggregate of microcrystalline clinoptilolites which is fringed with a film of smectite and low cristobalite. C. (Sample 439-16-3) Prismatic and tabular clinoptilolites filling the void of a dissolved glass shard which is fringed with a film of low cristobalite. D. (Sample 439-16-3) Prismatic and tabular clinoptilolites filling the void of a radiolarian shell which is transformed into opal-CT. E. (Sample 439-14-3, 40–43 cm) Prismatic and tabular clinoptilolites filling the void of a calcareous algae. Pores within the calcareous wall are completely filled with sparry calcite and a mixture of opal-CT and clay. Framboidal pyrite particles are seen. F. (Sample 439-28-3, 124–125 cm) A subangular clase of altered acidic vitric tuff in calcite–dolomite cemented lithic sandstone. Vitric shards in the tuff is altered to analcime, quartz, and chlorite. (Uppermost Oligocene section at a sub-bottom depth of 1063 meters in Hole 439.)*
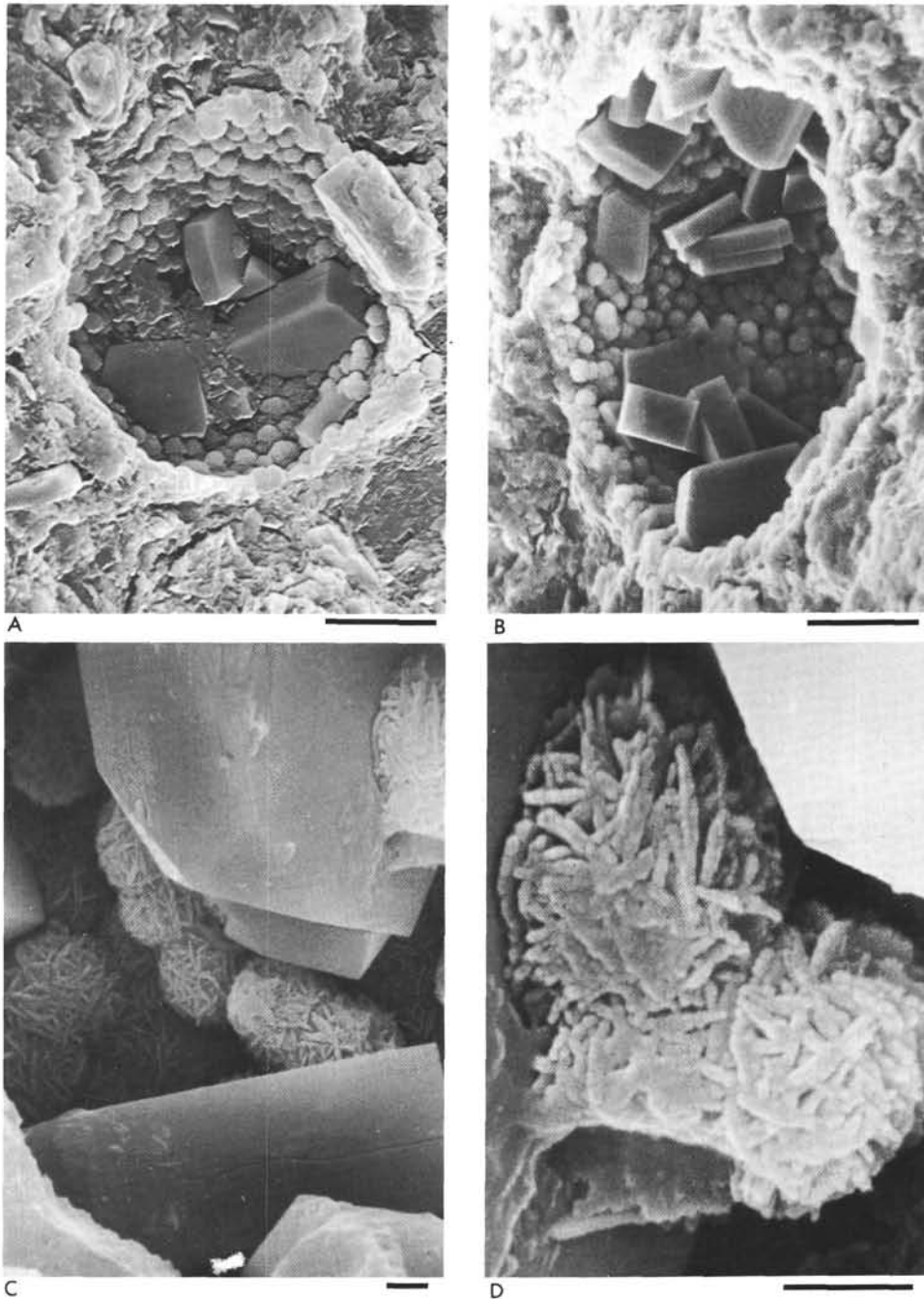
Figure 4. *Electron micrographs showing authigenic clinoptilolite crystals and opal-CT lepispheres in the void of radiolarian shells in tuffaceous, siliceous mudstone. (Lower Miocene section at a sub-bottom depth of 935 meters in Hole 439; Sample 439-14-3, 40–43 cm.) A. Tabular crystals of clinoptilolite are precipitated into the void of a radiolarian shell. Lepispheres of opal-CT cluster on the wall of the void. A hemilepisphere grows on the surface of clinoptilolite crystal. (Scale bar is 10 μm.) B. Tabular and prismatic clinoptilolites are crowded in the void. Opal-CT lepispheres cluster on the wall of a radiolarian shell (Scale bar is 10 μm.) C. Opal-CT lepispheres that consist of aggregates of minute rods grow in the interspace of clinoptilolites. (Scale bar is 1 μm.) D. Enlarging the upper-right corner of C. A hemilepisphere and a mushroomlike lepisphere of opal-CT grow on the surface of clinoptilolite. (Scale bar is 1 μm.)*
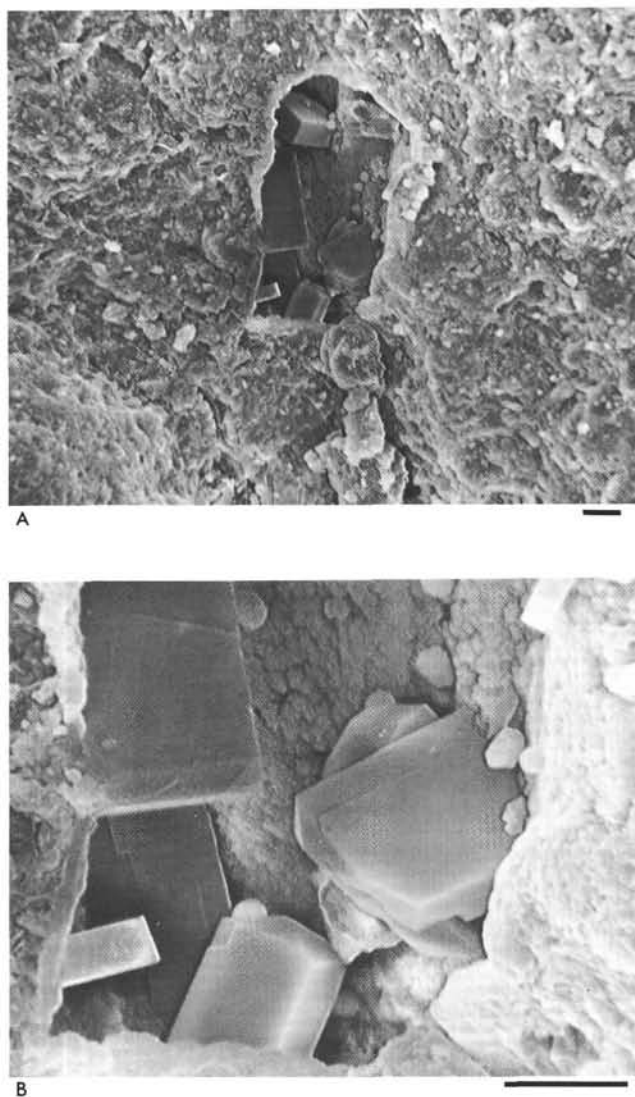
Figure 5. *Electron micrographs of authigenic clinop-tilolites filling the void of a dissolved glass shard in tuffaceous, siliceous mudstone. (Lower Miocene section at a sub-bottom depth of 735 meters in Hole 439; Sample 439-14-3, 40-43 cm; each scale bar is 10 μm.) A. Tabular and prismatic clinoptilolites protrude into the void from a fringe composed of low cristo-balite. Some lepispheres grow on the fringe and on the surface of clinoptilolites. B. Enlargement of the lower part of the void. The wall of the void is covered with a mosslike aggregate of tiny needles of low cris-tobalite. A hemilepisphere grown on the pyramidal surface of a prismatic crystal of clinoptilolite.*

TABLE 1
Chemical Composition of Clinoptilolites
in the Lower Miocene Tuffaceous, Siliceous
Mudstone from Sample 439-14-3, 40-43 cm

	1[a] (%)	2[b] (%)	3[c] (%)
SiO_2	69.52	68.45	66.53
Al_2O_3	12.59	13.54	12.96
Fe_2O_3 (total Fe)	0.17	0.13	0.07
MgO	0.24	0.21	0.28
CaO	0.45	0.49	0.37
Na_2O	1.19	0.80	1.06
K_2O	3.54	3.72	3.80
Total	87.70	87.34	85.07

Numbers of ions on the basis of 72(0)

Si	30.20	29.88	29.88
Al	6.45	6.97	6.86
Fe^{III}	0.05	0.04	0.02
Mg	0.16	0.14	0.19
Ca	0.21	0.23	0.18
Na	1.00	0.68	0.93
K	1.96	2.07	2.18
$Si:Al + Fe^{3+}$	4.65	4.26	4.34
$2(Mg + Ca)+ Na + K$	3.70	3.49	3.85

[a] Mean of 6 crystals filling voids of radio-larian shells.
[b] Mean of 3 crystals filling voids of calcareous echinoid spines and foraminifers.
[c] Mean of 6 crystals filling voids of dissolved glass shards.

into account, we can assume the dominant cations to be Na. K is also prominent. No compositional zoning within single crystals was detected, but there is a slight difference in composition among the crystals. The $Si:(Al + Fe^{3+})$ ratio is highest (4.65) in radiolarian shell voids, intermediate (4.34) in dissolved glass voids, and lowest (4.26) in voids of calcareous organisms. This distinction corresponds to the association of authigenic silica minerals: There are abundant opal-CT lepispheres in the voids of radiolarians, and low cristobalite wall, and some lepispheres in dissolved glass voids, and a lack of silica minerals in the voids of calcareous organisms. There is no tendency for Ca to predominate in clinop-tilolites in this last category.

Optic Properties

Clinoptilolites occur in the form of tabular and pris-matic crystals as shown in the micrographs (Figure 3) and electron micrographs (Figures 4 and 5). They can be as long as 0.03 mm, with prismatic cleavage; the elonga-tion shows length-slow on a Lakeside mount. The mean refractive indice is 1.489 ± 0.002 and the birefringence very low. It is imposible to detect any difference in optic properties among the different occurrences.

X-Ray Diffraction and Thermal Stability

Clinoptilolites were concentrated in a centrifuge tube using heavy liquid of bromoform diluted with ethyl alcohol. A considerable number of impurities such as

showed a linear relation for the zerotime correction, so that volatilization of these elements did not occur on the measurements. However, a considerable amount of Na was volatilized even on 4-s exposure, indicating that alkalies and alkaline earths are deficient compared with Al (Table 1).

All clinoptilolites analyzed are undoubtedly high in alkalies and in silica varieties. Taking the volatilization

silica minerals and plagioclase remained, even after three separation procedures. The X-ray diffraction powder data for the concentrated clinoptilolite sample (460-16-3) are tabulated in Table 2. The d(330, 400) reflection is rather weak and broad. Other, weaker reflections are probably masked by the impurities.

The clinoptilolites show strong thermal resistance. The reflection at 8.95 Å is unchanged after heating at 250°C for 12 hours. It shifts to 8.89 Å, its intensity decreasing by half, after heating at 750°C for 11 hours (Figure 6). This thermal stability is due to high alkali and silica content, as Mumpton (1960) and Boles (1972) have pointed out.

TABLE 2
X-Ray Diffraction Powder Data for Clinoptilolites from Sample 439-16-3, 111–112 cm

$2\theta°$ [a]	$d(Å)$	I
9.87	8.95	10
11.17	7.914	3
19.07	4.650	2
22.30	3.983	3
22.46	3.955	2
22.76	3.904	2
26.03	3.420	2
30.11	2.965	2

Note: Internal standard: quartz. Radiation: Cukα, scan speed: 0.5°/min., chart speed: 400 mm/hr.
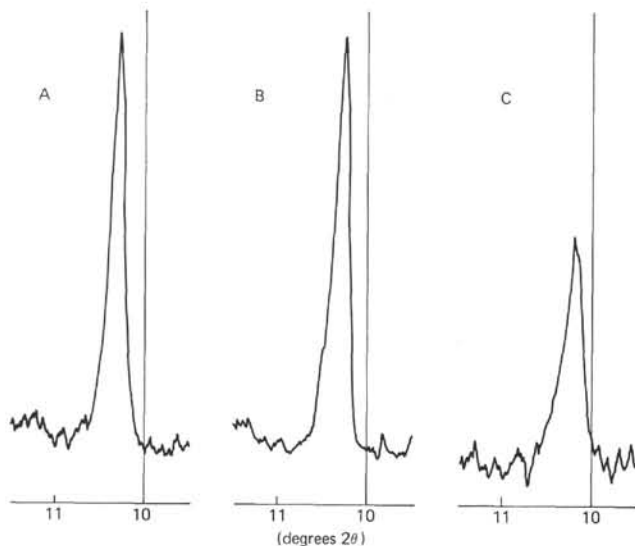
[a]Mean of 2 measurements.

Figure 6. *Thermal stability of clinoptilolites in Sample 439-16-3, 110–112 cm. A. Original. B. Heated at 250°C for 12 hours. C. Heated at 750°C for 11 hours.*

Authigenic Silica Minerals

Quartz and opaline silica coexist with clinoptilolite. Microscopic observation of thin sections reveals that quartz occurs as clastic grains and opaline silica as an alteration product of acidic glass fragments and remains of siliceous organisms such as diatoms, radiolarians, and sponge spicules.

Opaline silica was treated with a 20 per cent silicic hydrofluoric acid solution for 20 hours, then concentrated in a centrifuge tube using a heavy liquid of bromoform and ethyl alcohol solution. The X-ray diffraction powder pattern of one of the concentrated opaline silica samples (439-14-3) is illustrated in Figure 7. It is remarkable that two strong reflections are present at the d(101) position—4.099 Å and 4.055 Å. There are similar diffraction patterns in samples of lower and middle Miocene siliceous shales containing altered acidic glass fragments (Table 3). In the Miocene marine sections in northern Japan, opaline silica originating from biogenic opal in siliceous shales has a strong reflection within the range of 4.05 to 4.12 Å, associated with a weak reflection 4.33 Å, whereas opaline silica originating from altered acidic glass in zeolitized vitric tuffs has a strong reflection within the range of 4.04 to 4.05 Å; moreover, two types of opaline silica coexist in tuffaceous siliceous shales (Iijima and Tada, in press). Each of the examples is illustrated in Figure 8. The 4-Å-silica mineral of biogenic opal origin corresponds to the opal-CT identified by Jones and Segnit (1971), whereas that of altered glass origin is low cristobalite. The X-ray diffraction pattern and lithology of the samples are very similar to those of the tuffaceous, siliceous shales in northern Japan. For example, the siliceous shale contains two phases of silica, opal-CT and low cristobalite; the former is probably transformed from siliceous organisms whereas the latter is probably altered from acidic glass. In siliceous shale containing clinoptilolites (439-16-3), the majority of opal-CT occurs as a mass in the matrix mixed with clay particles. Opal-CT lepi-spheres of 2.5 to 3.5 μm in diameter cluster in the voids of radiolarian shells, some of them growing on clinoptilolites (Figure 4A and D). There is a low cristobalite fringe in the void of dissolved glass shard (Figure 5A). The wall of the void is covered with a mosslike aggregate of tiny needles of low cristobalite (Figure 5B). A few lepispheres are also found growing on clinoptilolites inside the voids of dissolved glass shards (Figure 5A and B). In this case, it is uncertain whether the lepispheres are opal-CT or low cristobalite.

Radiolarian shells are replaced by and filled with chalcedonic quartz in the Upper Cretaceous mudstone at a sub-bottom depth of 1145 meters (439-37-1, 56–58 cm). The elongation of chalcedonic quartz is length-fast.

Origin of Zeolites

Authigenic Clinoptilolite

Authigenic clinoptilolites have been found in two samples of lower Miocene tuffaceous, siliceous mud-
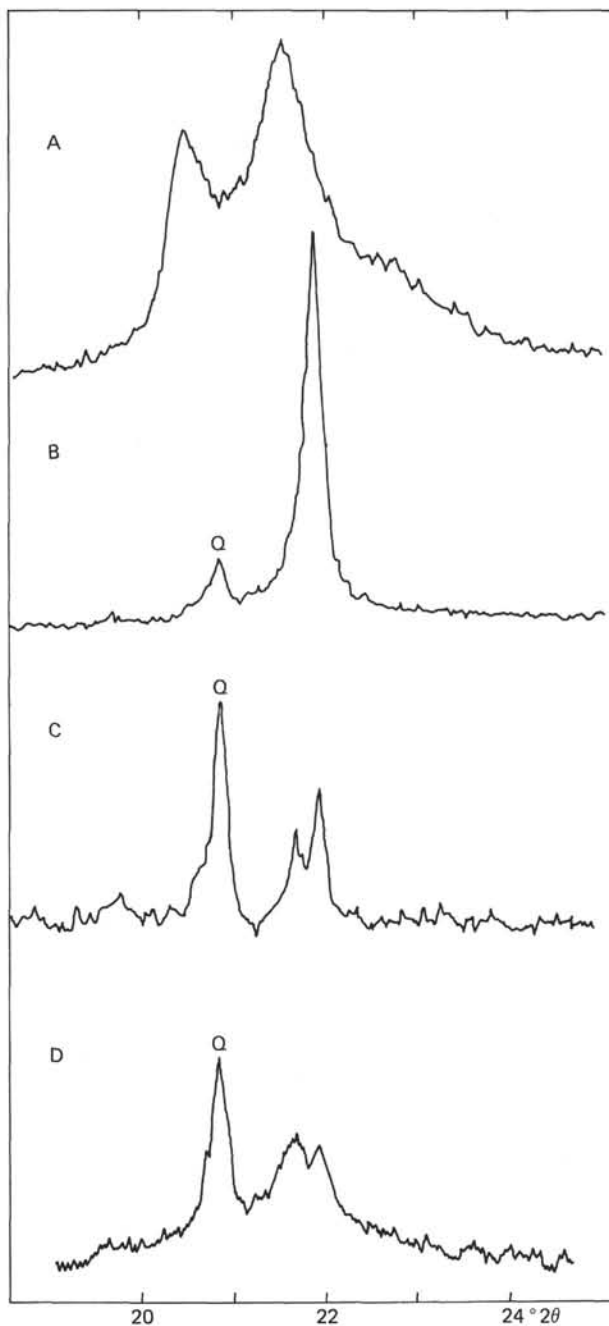
Figure 7. *X-ray diffraction powder patterns of authi-genic 4-Å silica minerals in siliceous shale, altered vitric tuff, and tuffaceous, siliceous mudstone. A. Opal-CT in a segregation vein in diatomaceous mud-stone of the Miocene Chokubetsu Formation, Toka-chi, southeast Hokkaido. (Sample AT77-189.) B. Low cristobalite with small amounts of pyroclastic quartz (Q) in zeolitized acidic vitric tuff of the Mio-cene Iwaya Formation, Takanosu, north Akita. (Sam-ple TK77-77.) C. Mixture of opal-CT and low cristo-balite with detrital quartz (Q) in tuffaceous, siliceous mudstone of the Miocene Funakawa Formation at a depth of 600 meters in the Shinonome AK-l Well, Akita. D. Concentrated silica minerals of lower Miocene tuf-faceous, siliceous mudstone at a sub-bottom depth of 735 meters in Hole 439. (Sample 439-14-3, 40-43 cm.)*

TABLE 3
The d(101) Spacing of 4-Å Silica Minerals from Selected Core Samples at Sites 438 and 439, DSDP Leg 57

Sample (Interval in cm)	Sub-bottom Depth (m)	$d(101)$ of Opal-CT (Å)	$d(101)$ of Low Cristobalite (Å)
438A-60-2, 59–61	622	–	–
438A-64-6, 134–135	668	–	–
438A-68-2, 24–26	700	4.11	4.05
438A-73-3, 58–60	749	4.10	4.053
438A-82-4, 100–102	835	4.097	4.051
438A-84-2, 126–128	852	4.10	4.048
438B-9-3, 58–61	904	4.09	4.048
439-11,CC	912	4.10	4.044
439-14-3, 40–43	935	4.099[a]	4.055[a]
439-16-3, 110–112	950	4.10	4.059

Note: Internal standard: quartz. Radiation: CuKα; scan speed: 0.5°/min.; chart speed: 400 mm/hr.; the values for $d(101)$ spac-ing of Opal-CT and low cristobalite are the mean of 2 measure-ments; error is ±0.005 but ±0.01 for the values with two decimal places.
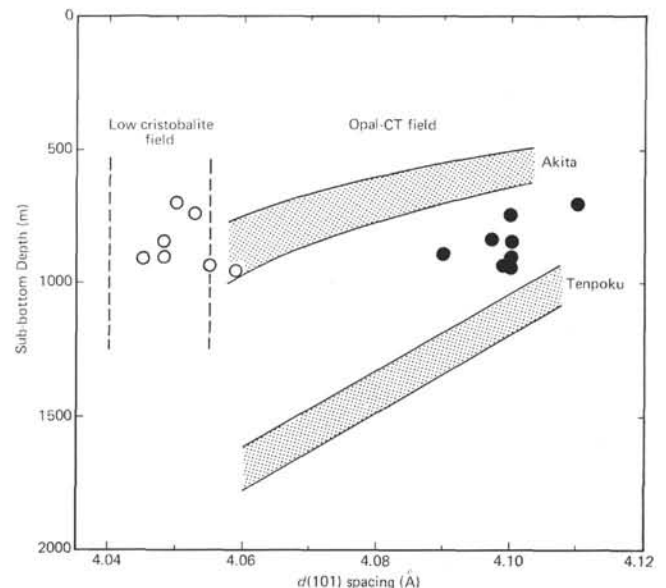
[a]Mean of 3 measurements.

Figure 8. *Relation of the d(101) spacings of diagenetic opal-CT (●) and low cristobalite (○) to the burial depth in siliceous shales, vitric tuffs, and tuffaceous, siliceous mudstones of Neogene sections at Sites 438 and 439. For comparison, the same relation in the deep wells of the Tenpoku and Akita oilfields (Iijima and Tada, 1980) is shown schematically as opal-CT and low cristobalite fields.*

stones at sub-bottom depths of 935 and 950 meters in Hole 439. They occur as euhedral crystals filling various voids of dissolved glass fragments, radiolarian shells, and calcareous organisms such as foraminifers and echi-noids. This mode of occurrence indicates precipitation from interstitial solution. The clinoptilolites are high in alkalies, expecially Na, and in silica varieties. The slight difference in chemical composition among them and the absence of compositional zoning suggest that the solu-tion remained homogeneous throughout the formation

of the porous, semi-indurated sediments. Nevertheless, the difference in their Si:(Al + Fe^{3+}) ratio and in the associated opaline silica indicates a change in chemical microenvironment. This change is probably caused by the presence of silica and alumina. The solution was undoubtedly oversaturated with low cristobalite — and probably with opal-CT as well — inside the voids of dissolved glass shards and with opal-CT inside the radiolarian shells because of the coprecipitation of these silica phases and of clinoptilolites. It is clear that some biogenic silica contributes to the clinoptilolites, especially those filling voids of radiolarian shells, where their Si:(Al + Fe^{3+}) ratio is significantly higher than in clinoptilolites occurring elsewhere. Alumina is more easily available from dissolved glass inside the voids of dissolved glass shards than inside the voids of micro-organic remains. Some of the Na, K, Ca, and Mg in the clinoptilolites may have originated from sea water trapped in the sediments.

Acidic glass fragments such as glass shards and pumice grains are found in many thin sections from the Pleistocene diatomaceous muds through the upper part of the lower Miocene siliceous mudstones. Pumice grains are partly altered to pale green to brownish green clay (probably montmorillonite) and isotropic opal, even in the Pleistocene section at the sub-bottom depth of 40 meters in Hole 438A. They are extensively altered — to aggregates of montmorillonite and low cristobalite — in the middle Miocene section at sub-bottom depths of more than 700 meters in Hole 438A and more than 850 meters in Hole 439; however, some glass fragments have remained fresh. In the lower Miocene section of Hole 439, they are completely altered to clinoptilolite, montmorillonite, and low cristobalite. We found no authigenic zeolites in the uppermost Oligocene sandstone section, in which no glass fragments, except for detrital clasts of analcimic tuff, are present. No zeolites are found in the Upper Cretaceous section in the bottom of Hole 439, which contains radiolarian shells but no glass fragments. The smooth surfaces of clinoptilolite crystals revealed by the SEM indicate that they are not etched by but equilibrate with or have been precipitated from the interstitial water. From the aforementioned data we conclude that the clinoptilolites are essentially derived from the reaction of acidic glass fragments with interstitial water at a depth of burial sufficient for elevated temperatures to accelerate the dissolution of glass, the diffusion of dissolved ions into voids, and the precipitation of clinoptilolites. According to the temperature measurements on board, it is 25.6°C at a sub-bottom depth of 957 meters in Hole 439. The calculated gradient is 24.7°C/km, assuming a temperature of 2°C on the sea floor. Consequently, present temperature at a sub-bottom depth of 935 meters — the shallowest occurrence of clinoptilolite — is estimated to be approximately 25°C.

Detrital Analcime

Fine-grained acidic vitric tuff, the glass fragments of which are completely altered to analcime, quartz, and chlorite, occurs sparsely, in the form of subangular clasts in lithic sandstones in the uppermost Oligocene section in Hole 439 (Figure 3F). The coarser grain size and angularity of the analcime-bearing tuff clasts and of the sandstone clasts indicate a nearby provenance, as we will discuss in detail in Part II. Similar analcimic tuffs are widespread in such thick Upper Cretaceous beds as the Hakobuchi Group and the Upper and Middle Yezo Groups in central Hokkaido west of the Hidaka Range (Iijima and Utada, 1972; Owa, 1975). Because the general tectonic trend in central Hokkaido is meridional, an offshore southward extension of Upper Cretaceous strata is expected. Furthermore, the abundance of authigenic chlorite, radiolarian shells replaced by chalcedonic quartz, and unaltered plagioclase grains in the sandstones is consistent with the degree of diagenetic alteration in the terrestrial Upper Cretaceous sequence, with its intercalations of analcime-bearing tuff. It is reasonable, therefore, to conclude that the tuff clasts were reworked from the Upper Cretaceous sediments near Site 439. The significant unconformity between the uppermost Oligocene and Upper Cretaceous sections at Site 439 supports this explanation (see site chapter for Sites 438 and 439).

Zeolitic Burial Diagenesis

Authigenic zeolites are widespread in altered acidic vitric tuffs and tuffaceous sediments of the thick marine and freshwater Cenozoic and Cretaceous sequences in the adjacent terrestrial areas of northern Japan. For example, clinoptilolite occurs in the Upper Cretaceous Kuji Group and the Paleogene Noda Group in the Kuji Coalfield of Iwate Prefecture (Iijima and Utada, 1972; Shimoyama and Iijima, 1976, 1977): Clinoptilolite, mordenite, analcime, heulandite, and laumontite are widely distributed in the Tertiary and Upper Cretaceous strata in central Hokkaido from Tenpoku through Hidaka (Iijima and Utada, 1972; Iijima, 1975, 1978; Owa, 1975; Shimoyama and Iijima, 1976, 1977). These zeolites exist in a vertically zonal arrangement that corresponds with the stratigraphic succession. Zone I is characterized by the absence of zeolites and the presence of fresh acidic glass; Zone II, by clinoptilolite and mordenite replacing the glass; Zone III, by analcime replacing the precursor zeolites; and Zone IV, by albite replacing the analcime (Iijima, 1978). The zones are vertical because, as we can deduce from deep borehole studies, from comparison with the degree of coalification, and from thermodynamic and synthetic studies (Iijima, 1975), burial diagenesis is mainly affected by the geothermal gradient. These zones belong to the Cenozoic and Upper Cretaceous sequence at Sites 438 and 439, as shown in Figure 9. The Quaternary through middle Miocene sections above the clinoptilolite-bearing horizon at a sub-bottom depth of 930 meters belong to Zone I. The lower Miocene section of Hole 439 corresponds to Zone II. The uppermost Oligocene section probably belongs to Zone II, regardless of the absence of clinoptilolite, for montmorillonite is common. Assignment of the Upper Cretaceous section at the bottom of Hole 439 to Zone III is based on the presence of common authigenic chlorite and quartz replacing radio-larian shells as well as of analcimic tuff clasts in the uppermost Oligocene sandstones, which were prob-
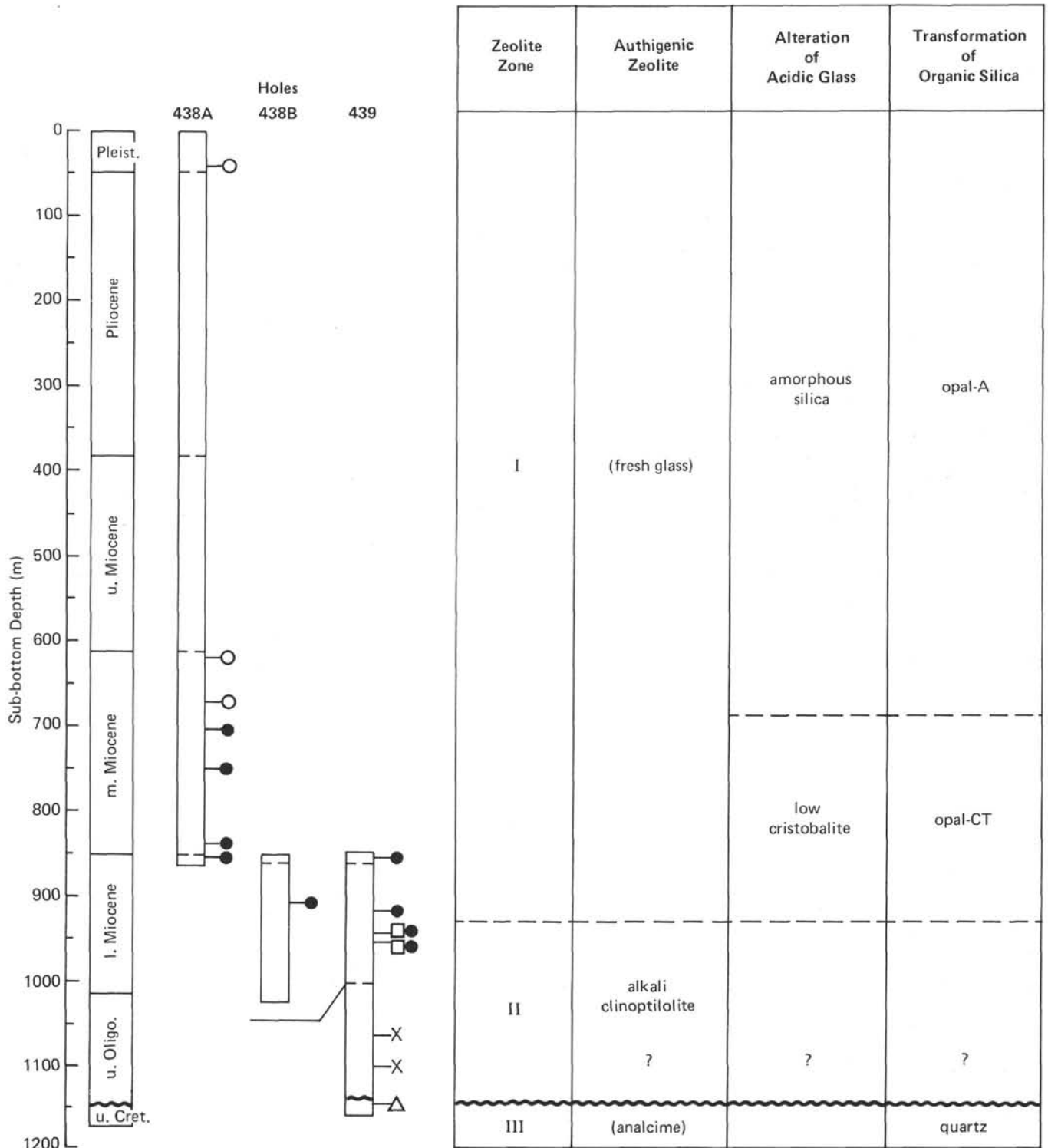
Figure 9. *Diagram showing the zeolite zones and the vertical zonal distribution of authigenic zeolite and silica minerals at Sites 438 and 439. Significant denudation probably occurred during the uppermost Oligocene–Upper Cretaceous interval represented by the unconformity. The occurrence of authigenic minerals and analcimic tuff clasts is marked in the following symbols: ○ amorphous silica, ● opal-CT and low cristobalite, △ quartz replacing radiolarian shells, □ clinoptilolite, and × analcimic tuff clasts.*

ably derived from the Upper Cretaceous strata, as we explained earlier.

The transitional temperature between each of the zones can be estimated from the depth of the boreholes in which burial diagenesis is progressing (Iijima and Utada, 1971; Iijima, 1978). On the one hand, the temperature is about 30°C at the boundary between Zones I and II in tuffaceous, diatomaceous shales of the late Miocene section in the MITI-Hamayuchi well in north-central Hokkaido. This is not inconsistent with about 25°C at the same boundary in similar lithogy of the middle to lower Miocene section in Hole 439. On the other hand, at the boundary between Zones II and III the temperature range is 84° to 91°C in the Neogene marine sections in four MITI boreholes. A comparison between the degree of coalification, as defined by vitrinite reflectance and the Krevalent band, and the zeolite zones in the Japanese Tertiary coalfields supports that temperature range (Shimoyama and Iijima, 1976, 1978). However, in Hole 439 the temperature is estimated to be approximately 30°C at the unconformity between the uppermost Oligocene and Upper Cretaceous sections, which is the boundary between Zones II and III. The clasts of analcime-bearing tuff in the uppermost Oligocene sandstones indicate that the analcitization had occurred in the pre-uppermost Oligocene sequence below the unconformity. Hence the discrepancy in temperature may be explained if that pre-uppermost Oligocene section, several kilometers thick, was denuded during the interval represented by the unconformity. Had the geothermal gradient been higher than at present, the denuded overburden would not have been as thick.

Silica Diagenesis

Clinoptilolites in tuffaceous, siliceous mudstones in the lower Miocene section in Hole 439 are associated with opal-CT and low cristobalite. As we discussed earlier, opal-CT is transformed from biogenic silica, whereas low cristobalite derives from acidic volcanic glass. Both siliceous organic remains and acidic glass fragments occur in tuffaceous, diatomaceous muds and mudstones from the Quaternary through lower Miocene sections. X-ray diffraction patterns of concentrated samples treated with dilute silicic hydrofluoric acid revealed the sub-bottom depth of the shallowest occurrence of opal-CT and low cristobalite to be 700 meters in Hole 438A and 851 meters in Hole 439. Pumice grains are extensively altered to montmorillonite and isotropic opaline silica even in the tuffaceous, diatomaceous mud in the Pleistocene section at a sub-bottom depth of 40 meters in Hole 438A. However, isotropic opal is X-ray amorphous. Although diatom frustules are considerably dissolved in the diatomaceous mudstones in the upper part of the middle Miocene section in Hole 438A, opaline silica — which probably corresponds to the opal-A of Jones and Segnit (1971) — is X-ray amorphous. These findings may be explained by the fact that the amorphous opaline silica originating in both altered acidic glass and biogenic silica is transformed into low cristobalite and opal-CT, respectively, at a depth at which temperature becomes sufficiently high. The temperature measured on board is

26°C at a sub-bottom depth of 868 meters in Hole 438A. The calculated gradient is 27.6°C/km, assuming a sea floor temperature of 2°C. Consequently, the temperature is estimated to be 21°C at present at a sub-bottom depth of 700 meters — the shallowest occurrence of opal-CT and low cristobalite. Silica phases precede clinoptilolite — a general rule in the Neogene sections in northern Japan (Iijima and Tada, in press).

Low cristobalite is altered from acidic volcanic glass, whereas opal-CT originates from biogenic silica. These derivations are generally recognizable in altered vitric tuffs, siliceous shales, and tuffaceous, silliceous shales of the Tertiary and Upper Cretaceous sections in northern Japan; minor elements such as Al, Na, K, and Ca are significant in low cristobalite, whereas they are absent or in trace amounts only in opal-CT (Iijima and Tada, in preparation). The difference in composition clearly reflects the composition of the original materials and probably affects the crystal structure of the silica phases.

The change of $d(101)$ spacing of opaline silica is considered useful for estimating the degree of burial diagenesis and is principally affected by heating (Murata and Larson, 1975; Murata and Randall, 1975; Murata et al., 1977; Mizutani, 1977; Mitsui and Taguchi, 1977). In fact, as shown schematically in Figure 8, the $d(101)$ spacing of opal-CT in siliceous shales of the Miocene sections in deep wells in the Tenpoku and Akita oilfields, northern Japan, decreases downward within a range of 4.05 to 4.11 Å. The change of $d(101)$ spacing of opal-CT in siliceous mudstones of the middle and lower Miocene sections in Holes 438A and 439 varies within a range of 4.09 to 4.11 Å, which corresponds to that of the shallower part of the wells. However, the change of $d(101)$ spacing of low cristobalite in altered vitric tuffs and tuffaceous sediments is limited within the range of 4.04 to 4.06 Å; nor does it show any relation to burial depth.

The progressive decrease — or progressive ordering — in the $d(101)$ spacing of opal-CT probably takes place in two ways. First, the disordered opal-CT with a wide spacing which forms at the depth of the shallowest occurrence becomes ordered as temperatures rise with an increase in depth. Second, opal-CT with a narrower spacing is precipitated into voids at greater depths and at higher temperatures than the shallowest occurrence. The opal-CT lepispheres that grow on clinoptilolites in voids of radiolarian shells in tuffaceous siliceous mudstones at a sub-bottom depth of 935 meters in Hole 439 (Figure 4A and D) clearly prove the second case. The relationship between zeolite and silica diagenesis is shown in Figure 9.

Radiolarian shells are replaced by and filled with chalcedonic quartz in the Upper Cretaceous mudstone at a sub-bottom depth of 1145 meters in Hole 439. In the Miocene sections in northern Japan, opal-CT originating in biogenic silica is completely transformed into chalcedonic quartz in Zone III, the analcime zone (Iijima and Tada, in press). It is probable that the silicification of radiolarian shells occurred parallel to the diagenetic change of acidic vitric tuffs into the anal-

cime-quartz-chlorite rock from which the analcime-bearing tuff clasts were reworked into the overlying uppermost Oligocene sandstones.

PART II. SANDSTONE PETROGRAPHY

In Part II, the uppermost Oligocene and Upper Cretaceous sandstones at Site 439 are described petrographically and their provenance discussed. Clasts of the younger sediments at Sites 438 and 439 are also treated briefly. The stratigraphy of the samples analyzed is illustrated in Figure 2.

Petrographic Description

Thin sections were made from six samples of sandstone, perpendicular to bedding planes. They were observed under a petrographic microscope. The modal composition was calculated from the point-counter analyses (Table 4 and Figure 10).

Upper Cretaceous Sandstone

This sandstone is chlorite-calcite-cemented, fine-grained, argillaceous, and feldspathic (Sample 439-37-1, 56–58 cm). It occurs as thin gray laminae in dark gray, radiolarian-bearing, carbonaceous mudstone. Sand grains are well sorted, ranging in size from 0.04 to 0.25 mm; the majority are 0.1 to 0.15 mm, with angular to subrounded shapes. They are made up largely of quartz and feldspars with small amounts of mica and lithic fragments. Accessories are multicolored (bluish green and brown) tourmaline and epidote.

Quartz grains are clear. Most of them contain fluid inclusions, and some contain rutile needles. Plagioclase grains are dominantly fresh, clear oligoclase to andesine ($An_{28}Ab_{72}$–$An_{33}Ab_{67}$) and subordinately turbid, dusty albite (An_5Ab_{95}–$An_{10}Ab_{90}$) with sericite inclusions. Dus-ty orthoclase and microcline are rare. Mica flakes are brown biotite with a small amount of muscovite and green chloritized biotite. Because the flakes are arranged in parallel to bedding planes, they are extensively distorted by the overburden. Lithic fragments are composed of chalcedonic chert, metaquartzite, mudstone, altered tuff, and acidic volcanics. Chalcedony fragments, probably derived from chert veins, with a featherlike texture are not uncommon.

Fossils content consists of small amounts of black carbonaceous fragments and radiolarian shells. The shells, with a diameter of 0.12 to 0.24 mm, are replaced by a radial aggregate of chalcedonic quartz which is length-slow. Shell voids are filled with pale green glauconite, chalcedonic quartz, and pyrite.

Calcite not only cements but also replaces sand grains, especially and extensively in plagioclase. It occurs as a mosaic aggregate of coarse, sparry crystals made up of several grains. Pale green aggregates of microcrystalline chlorite fill the interstices.

Uppermost Oligocene Sandstones

Oligocene sandstones are fine to coarse grained and massive. The carbonate-cemented part of the sandstone section is light gray and indurated, the noncemented part gray and friable. Grain size tends to decrease upward and sorting to improve (Figure 11). Roundness is variable in different lithologies, but tends to increase upward. Lithic fragments are always predominant, ranging from 56 per cent of the sand grains in the upper part of the sandstone section to 82 per cent in the lower part. The clay matrix is more than 25 per cent of sandstones, except for 3 per cent in Sample 439-28-3 which is cemented and replaced by carbonates. Thus the sandstone type corresponds to the "lithic graywacke" of Pettijohn, Potter, and Siever (1972).

TABLE 4
Modal Analyses of the Upper Cretaceous and Uppermost Oligocene Sandstones at Site 439, DSDP Leg 57

	Sample (Interval in cm)					
	439-37-1, 56–58	349-32-1, 99–101	439-31-4, 43–45	439-30-3, 15–18	439-28-3, 124–125	439-26-5, 117–119
Sand grains						
Quartz	47.4	9.5	13.2	11.4	10.5	20.1
Feldspar	34.2	8.3	8.0	13.2	14.9	24.3
Biotite	3.8	tr	tr	—	tr	tr
Chert and siliceous shale	7.4	34.0	44.1	31.3	4.7	7.0
Carbonate rocks and flint	—	12.0	12.5	14.1	4.2	0.3
Mudstone	4.1	20.1	17.1	15.4	18.7	10.9
Tuff	1.9	1.0	0.6	0.5	1.8	0.2
Acidic volcanics	1.2	15.1	4.5	14.1	45.2	37.2
	100.0	100.0	100.0	100.0	100.0	100.0
Sand grains	51.5	56.8	53.7	59.7	61.9	71.5
Clay matrix	40.0	24.5	34.0	34.2	3.0	26.0
Carbonate cement	8.5[a]	10.6	10.5	2.4	34.1[a]	—
Pore	—	8.1	1.8	3.7	1.0	2.5
	100.0	100.0	100.0	100.0	100.0	100.0

Note: Numerals represent percentage.
[a] Includes significant amounts of replacement calcite.
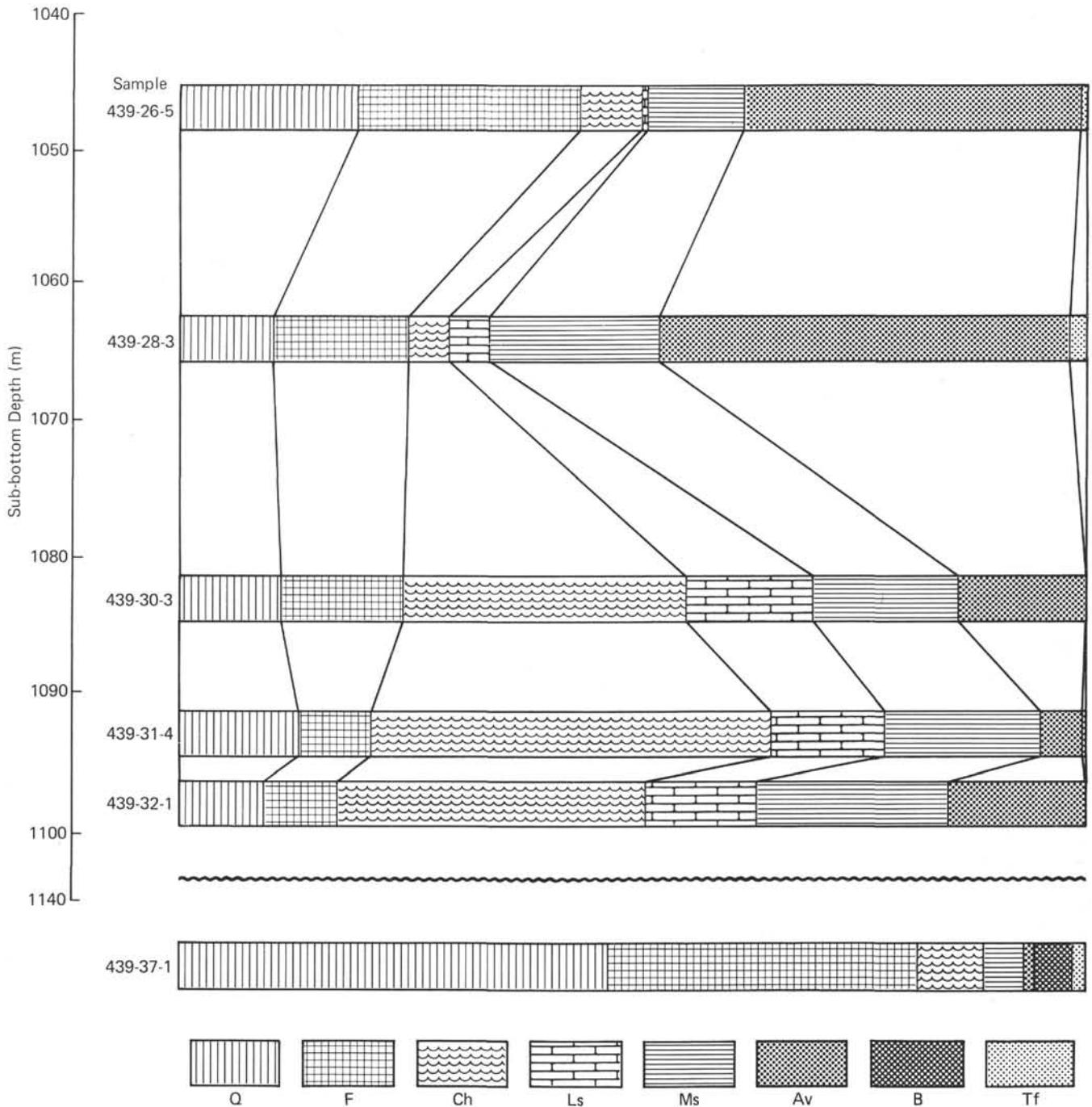
Figure 10. *Modal grain composition of the Upper Cretaceous and uppermost Oligocene sandstones in Hole 439. (Q = quartz, F = feldspar, Ch = chert and siliceous shale, Ls = limestone and dolostone, Ms = mudstone, Av = acidic volcanics, B = biotite, and Tf = tuff.)*

Lithic fragments can be classified into three groups, based on provenance. The first group is older sedimentary rock and weakly metamorphosed rock, including chert, siliceous shale, limestone, dolostone, flint, clay slate, and metamorphosed basic lava. The second group is younger sedimentary rock such as mudstone, carbonaceous shale, arkosic sandstone, ankeritic rock, and altered tuff. The third group is acidic volcanic rock similar to the dacite gravels in the basal conglomerate.

The younger rocks are common — 16 to 22 per cent of the sand grains — as subangular to rounded clasts throughout the sandstone section. The older rocks — above all, chert and siliceous shale — are abundant — 45 to 60 per cent of the sand grains — as angular, coarse clasts in the lower part of the section (Figure 12). In addition the acidic volcanic rocks are prominent — 35 to 45 percent of the sand grains — as angular to rounded clasts in the upper part of the section.
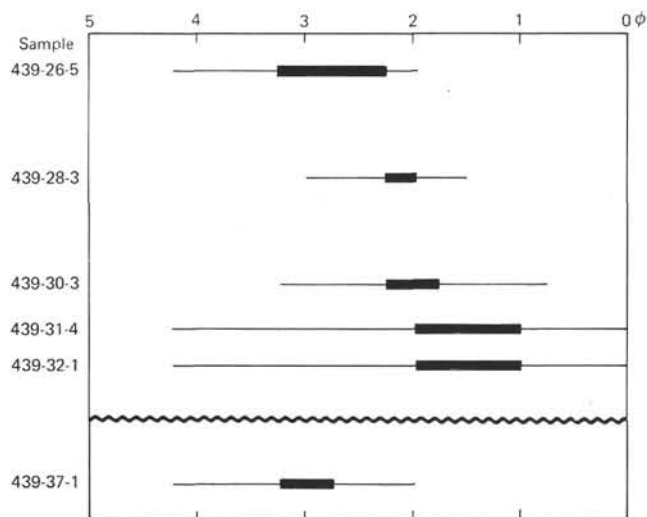
1155

Figure 11. *Grain-size distribution of the Upper Creta-
ceous and uppermost Oligocene sandstones in Hole
439, estimated under the microscope. (Solid bars rep-
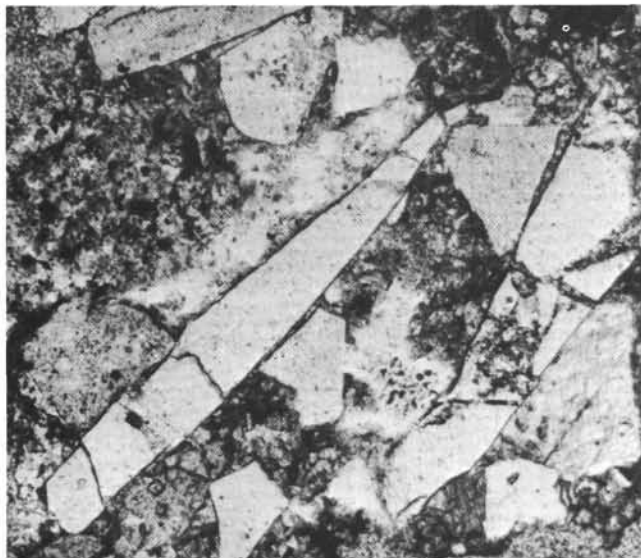resent the dominant grade.)*

Figure 12. *Angular clasts of chalcedonic chert (light
gray) and subangular to rounded clasts of carbonaceous
mudstone (gray, dusty) in the uppermost Oligocene
sandstone. (Sample 439-31-4, 43–45 cm; vertical side
is approximately 1 mm; unpolarized light.)*

Older Sedimentary Rock and Metavolcanics

Chert: gray and rarely red, chalcedonic, sometimes
containing radiolarian shells and chalcedony veinlets.
Siliceous shale: mixture of cryptocrystalline chalcedonic
quartz and clay, frequently including radiolarian shells.
Limestone: finely to coarsely crystalline, occasionally
dolomitic. **Dolostone:** finely to coarsely crystalline.
Flint: chalcedonic, containing micritic calcite and dolo-
mite rhombohedra. **Clay slate:** illitic and chloritic, with
slaty cleavage. **Green rock:** metavolcanics consisting of
chlorite, albite, and quartz.

Younger Sedimentary Rock

Mudstone: dark gray to gray, semi-indurated, con-
sisting of various amounts of silt-sized quartz and
feldspar in pale brown to greenish brown clay matrix.
Carbonaceous shale: dark gray to dark brownish gray,
semi-indurated, containing abundant flakes of carbona-
ceous matter. **Arkosic sandstone:** fine grained, con-
sisting of biotite, dusty oligoclase, and quartz. **Ankeritic
rock:** pale brown to brown aggregates of ankerite rhom-
bohedra. **Altered vitric tuff:** (see Part I).

Acidic Volcanic Rock

Rhyolitic rock: white, consisting of tiny plagioclase
laths and devitrified glass altered to aggregates of
chalcedonic quartz and orthoclase. **Dacitic rock:** light
gray to black and brown; consisting of plagioclase laths
and intersertal colorless to dark brown glass, the laths
frequently arranged subparallel to each other.

Quartz and feldspar grains are angular to subangu-
lar. They tend to increase upward along with dacite
clasts, from 18 per cent to 44 per cent of the sand grains.
There are three types of quartz grains: clear, single
crystals with fluid inclusions; single crystals or com-
posite grains showing wavy extinction; and fibrous chal-
cedony fragments. The clear, single crystal grains in-
crease along with dacite clasts in the upper part of the
section. Two types of plagioclase grains are distin-
guished: dusty sodic plagioclase ($\sim An_{10}Ab_{90}$), common-
ly with sericite inclusions and clear plagioclase ($An_{23}
Ab_{77}$– $An_{50}Ab_{50}$), frequently with zonal structure. The
first type is common in the lower part of the section,
where older sedimentary rock clasts are dominant. The
second type, on the contrary, is abundant in the upper
part of the section, where dacite clasts increase. The mi-
nor and accessories are dusty orthoclase, biotite, chlo-
rite, zircon, multicolored (bluish green and brown) tour-
maline, apatite, sphene, iron opaques, and leucoxene.

The uppermost Oligocene sandstones are frequently
cemented with dolomite rhombohedra and sparry cal-
cite as described in the chapter on carbonate diagenesis
by Matsumoto and Iijima (this volume). The calcite not
only cements but also extensively replaces sand grains
such as plagioclase and dacite clasts. The matrix is as
much as 34 per cent, consisting of montmorillonitic and
illitic clay. Authigenic glauconite pellets and plant
fragments occur sparsely in the upper part of the sand-
stone section.

Clasts in Neogene and Pleistocene Siliceous and Diatomaceous Deposits

Clasts in siliceous and diatomaceous deposits of the
Neogene and Pleistocene sections at Sites 438 and 439
are exclusively of acidic volcanic origins except for chert
fragments in the lower Miocene sandy siliceous shale.
Angular clear quartz, clear plagioclase (oligoclase to
andesine), glass shards, pumice grains, and dacitic rock
fragments are scattered. The minor and accessories are
biotite, green hornblende, augite, and zircon. Plant
fragments occur sparsely in the lower Miocene section.

Provenance of Sandstones

In this section our main concern is the provenance of uppermost Oligocene sandstones. They were undoubtedly deposited in a shallow environment, as the close association with unconformity and shallow molluscan shells testify.

Angular clasts of older sedimentary rock are the main components of the medium- to coarse-grained lithic sandstones in the lower part of the section. The older sedimentary rocks, including radiolarian chert, siliceous shale, limestone, dolostone, flint and clay slate, and metabasic volcanics, correspond to the lithologic assemblage of the lower Mesozoic to upper Paleozoic Sorachi Group in south-central Hokkaido. However, the angular shape and coarseness of the clasts and the common occurrence of carbonate rock fragments in the sandstones (Figure 12) make as remote a provenance as south-central Hokkaido unlikely. A more probable source is the offshore southward extension of the Sorachi Group to as far south as Site 439, for the general trend in central Hokkaido is north–south. Iijima's and Kagami's (1961) theory that the Hidaka metamorphic zone occupying the main part of the Hidaka Range extends southward off Sanriku was based on the study of dredge and trawl samples collected from Site JEDS-2-$S_{1,2}$ at a water depth of 2330 to 2350 meters off Onagawa, south of Sanriku, by *Ryof-umaru* during the Second Japanese Expedition of the Deep Sea. Furthermore, on the basis of the paleogeological and paleogeographical study of Hokkaido in the Paleogene, Iijima (1964) considered that the Kamuikotan tectonic zone — including the Sorachi Group, glaucophanitic metamorphics, and serpentinite — extends southward off Sanriku. The basement of the "Oyashio ancient landmass" (1978, *Geotimes,* 23 [No. 4], 18) is probably the southern extension of the Sorachi Group, from which the angular clasts of the uppermost Oligocene sandstones would derive.

Other prominent components of the lower part of the sandstone section are clasts of younger sedimentary rock including mudstone, carbonaceous shale, and altered acidic vitric tuff containing analcime. Such a lithologic assemblage corresponds to the Upper Cretaceous Hakobuchi, Upper Yezo, and Middle Yezo Groups in south-central Hokkaido. The Middle Yezo Group covers the Sorachi Group with clinounconformity in the Hidaka coastal district (Kimura et al., 1975). However, the general trend of the Upper Cretaceous strata is north–south, so that a southward offshore extension together with the underlying Sorachi Group is probable. The Upper Cretaceous marine shale at the bottom of Hole 439 is considered part of the extension. As discussed in Part I, an overburden several kilometers thick must have overlain the marine shale and been denuded before the deposition of the uppermost Oligocene sediments. The clasts of younger sedimentary rocks were apparently reworked from the Upper Cretaceous overburden. Clasts of younger rock are rounder than those of the older rock, probably because of the difference in degree of induration.

Acidic volcanic clasts become predominant in the upper part of the uppermost Oligocene sandstone section. They probably originated from the volcanic high which supplied the basal conglomerate with dacite gravels. However, it is curious that there are only a few volcanic clasts in the lower part of the section overlying the dacite conglomerate.

CONCLUSION

We conclude with a geologic history of Sites 483 and 439. The equivalents of the lower Mesozoic and upper Paleozoic Sorachi Group and the overlying Upper Cretaceous strata extend southward off Sanriku adjacent to Site 439. They were upheaved and denuded during the Paleogene, preceding the uppermost Oligocene transgression. The amount of denudation is estimated to be approximately several kilometers at Site 439, on the basis of the discontinuity in the zeolite zoning due to burial diagenesis at the unconformity between the Upper Cretaceous and uppermost Oligocene sections. Most clasts of the uppermost Oligocene sandstones derived from a nearby provenance consisting of both older and younger sedimentary rocks and of penecontemporaneous dacite volcanics. The deposition of diatomaceous muds intermingled with pyroclastic material prevailed during the Miocene and Pliocene. Present-day burial diagenesis causes the formation of clinoptilolite from acidic glass shards at sub-bottom depth of 935 meters in Hole 439 at a temperature of about 25°C. It also causes the transformation of opal-CT from biogenic silica and of low cristobalite from acidic glass at a sub-bottom depth of 700 meters in Hole 438A at a temperature of about 21°C.

REFERENCES

Bence, A. E., and Albee, A. L., 1968. Empirical correction factors for the electron microanalysis of silicates and oxides. *J. Geol.,* 76, 382–403.

Boles, J. R., 1972. Composition, optical properties, cell dimensions, and thermal stability of some heulandite group zeolites. *Am. Mineral.,* 57, 1463–1493.

Iijima, A., 1964. The Paleogene paleogeology and paleogeography of Hokkaido. *Japan J. Geol. Geogr.,* 35, 43–55.

————, 1975. Effect of pore water to clinoptilolite analcime–albite reaction series. *J. Fac. Sci., Univ. Tokyo,* 19, 133–147.

————, 1978. Geological occurrences of zeolite in marine environments, *In* Sand, L. B., and Mumpton, F. J. (Eds.), *Natural Zeolites: Occurrence, Properties, Use:* Oxford and New York (Pergamon Press), pp. 175–198.

Iijima, A., and Kagami, H., 1961. Cenozoic tectonic development of the continental slope, northeast of Japan. *J.Geol. Soc. Japan,* 67, 561–577.

Iijima, A., and Tada, R., in press. Silica diagenesis of Neogene diatomaceous and volcaniclastic sediments in northern Japan. *Sedimentology.*

Iijima, A., and Utada, M., 1971. Present-day zeolitic diagenesis of the Neogene geosynclinal deposits in the Niigata oil field, Japan. *Molecular Sieve Zeolites—I, Advances in Chem. Ser.,* 101, 342–349.

————, 1972. A critical review on the occurrence of zeolites in sedimentary rocks in Japan. *Japan. J. Geol. Geogr.,* 42, 61–84.

Jones, J. B., and Segnitt, E. R., 1971. The nature of opal. I. Nomenclature and constituent phases. *J. Geol. Soc. Aust.,* 18, 57–68.

Kimura, T., Yoshida, S., and Toyohara, F., 1975. Significance of unconformity between Yezo and Sorachi Groups. *GDP Circular* II-1-(1), No. 3, pp. 29–38.

Mitsui, K., and Taguchi, K., 1977. Silica mineral diagenesis in Neogene Tertiary shales in the Tenpoku district, Hokkaido, Japan. *J. Sed. Petrol.,* 47, 158–167.

Mizutani, S., 1977. Progressive ordering of cristobalitic silica in the early stage of diagenesis. *Contrib. Mineral. Petrol.,* 61, 129–140.

Mumpton, F. A., 1960. Clinoptilolite redefined. *Amer. Mineral.,* 45, 351–369.

Murata, K. J., Friedman, I., and Gleason, J. D., 1977. Oxygen isotope relations between diagenetic silica minerals in Monterey Shale, Temblor Range, California. *Amer. J. Sci.,* 277, 259–272.

Murata, K. J., and Larson, R. R., 1975. Diagenesis of Miocene siliceous shales, Temblor Range, California. *J. Research U.S. Geol. Survey,* 3 (No. 5), 553–566.

Murata, K. J., and Randall, R. G., 1975. Silica mineralogy and structure of the Monterey Shale, Temblor Range, California. *J. Research U.S. Geol. Survey,* 3 (No. 5), 567–572.

Oehler, J. H., 1975. Origin and distribution of silica lepispheres in porcellanite from the Monterey Formation of California. *J. Sed. Petrol.,* 45 (1), 252–257.

Owa, I., 1975. Zeolitic diagenesis of the Cretaceous sediments in the central–axial part of Hokkaido, Japan [M.A. thesis]. Geological and Mineralogical Institute, Hokkaido University, pp. 1–81.

Pettijohn, F. J., Potter, P. E., and Siever, R., 1972. *Sand and Sandstone:* Berlin (Springer-Verlag), p. 618.

Shimoyama, T., and Iijima, A., 1976. Influence of temperature on coalification of Tertiary coal in Japan (summary). *Assoc. Am. Petrol. Geol. Memoir,* 25, 15–22.

————, 1977. Organic and mineral phases in burial diagenesis. *Prof. K. Huzioka Mem. Volume:* Akita (Fuzioka Kazuo Kyoju Taikan Kinen Kai), pp. 131–149.

————, 1978. Influence of temperature on coalification of Tertiary coal in Japan. *Memoirs Geol. Soc. Japan,* 15, 51–67.